

Random walks of a quantum particle on a circle

N Fjeldsø, J Midtdal and F Ravndal

Department of Physics, University of Oslo, N-0316 Oslo 3, Norway

Received 12 October 1987

Abstract. When the quantum planar rotor is put on a lattice its dynamics can be approximated by random walks on a circle. This allows for fast and accurate Monte Carlo simulations to determine the topological charge of different configurations of the system and thereby the θ dependence of the lowest energy levels.

1. Introduction

Non-Abelian gauge theories like QCD have configuration spaces of highly non-trivial topologies due to local gauge invariance which identifies points in this abstract space. When these theories are quantised one is led to introduce an unknown angle θ [1]. Physical quantities like the vacuum energy and particle masses will in general depend on it. Like most other properties of these theories, this dependence cannot in general be established using ordinary perturbative methods. Recently attempts have been made to use numerical methods instead, based on Monte Carlo simulations of the corresponding lattice gauge theories [2]. These calculations are time consuming and only very small lattices have been considered.

In order to get a better understanding of these effects and also the numerical problems involved, we want to consider the simplest possible system where the θ dependence is most directly accessible. This is the planar rotor, or a free particle on a circle [3]. Although this is almost a trivial system it can be used to model the spectrum of certain molecules [4] and the motion of electrons in a circular SQUID [5].

In the next section we will use the path integral formalism to relate the topological angle θ to the winding number Q of the closed trajectories of the particle moving in imaginary time on a circle. One can easily find all energy levels and correlation functions of interest. For numerical simulations one must discretise the time variable. This is done in § 3, where the particle is allowed to move on a finite lattice. Even in this case one can obtain an exact result for the ground-state energy by approximating the quantum paths with random walks. In this approximation, which is exact when the lattice spacing goes to zero, one can also very naturally simulate the quantised motion of the particle. The path integrals will just be sums over sufficiently large numbers of ordinary random walks. This allows for a fast and most direct method to calculate all quantum mechanical expectation values. We first obtain accurate results for the ground-state energy by this method. From the two-point correlation function we also find the energy of the first excited state as a function of the angle θ . This corresponds to the mass gap in lattice gauge theories. In the final section we discuss the obtained results, and also how this particular Monte Carlo algorithm can be useful in other situations.

2. Quantum mechanics of the planar rotor

A particle on a circle with angular variable ϕ has the Lagrangian $L = \frac{1}{2}\dot{\phi}^2$ in appropriate units. The conjugate momentum is $p_\phi = \dot{\phi}$ and the Hamiltonian $H = \frac{1}{2}p_\phi^2$. When the motion is quantised, the momentum becomes the operator $p_\phi = (1/i)(d/d\phi)$ with normalised eigenfunctions $\psi_k(\phi) = (1/2\pi)^{1/2} \exp(ik\phi)$. The constant k is determined by the boundary conditions. If the eigenfunctions are required to be strictly periodic, i.e. $\psi_k(\phi + 2\pi) = \psi_k(\phi)$, then $k = n = 0, \pm 1, \pm 2, \dots$. The corresponding energy eigenvalues are $E_n = \frac{1}{2}n^2$. This is the standard textbook result for a planar quantum rotor.

One can also consider the more general case when one only requires the probability density $\rho(\phi) = |\psi(\phi)|^2$ to be periodic. This makes it possible to introduce a phase θ such that

$$\psi(\phi + 2\pi) = \exp(-i\theta)\psi(\phi). \tag{2.1}$$

The angular momentum now takes the values $k = n - \theta/2\pi$ and the corresponding eigenfunctions are $\psi_n(\phi) = (1/2\pi)^{1/2} \exp[i(n - \theta/2\pi)\phi]$. With the same Hamiltonian as above, the energy eigenvalues are then $E_n(\theta) = \frac{1}{2}(n - \theta/2\pi)^2$. The lowest ones are shown in figure 1. In particular, we see that the ground-state wavefunction is $\psi_\theta = \psi_0(\phi)$ with energy $E_\theta = \theta^2/8\pi^2$ when $0 \leq \theta < \pi$. It changes abruptly into $\psi_\theta = \psi_1(\phi)$ with energy $E_\theta = (2\pi - \theta)^2/8\pi^2$ for $\pi \leq \theta < 2\pi$.

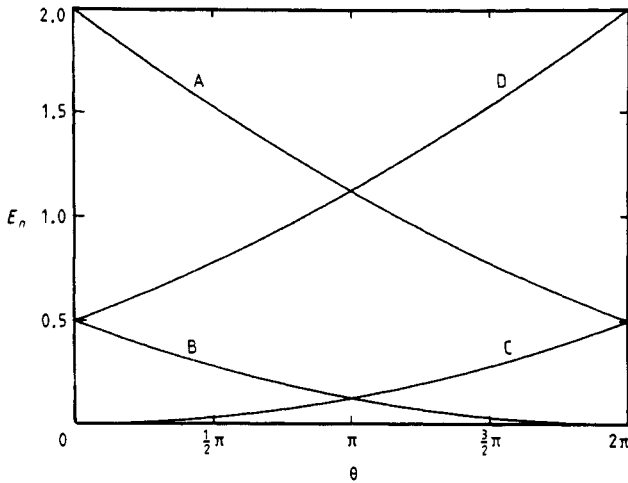


Figure 1. Lowest energy levels of the planar rotor. $n = 2$ (A), 1 (B), 0 (C), -1 (D).

It is convenient to have periodic wavefunctions $\psi(\phi + 2\pi) = \psi(\phi)$ instead of (2.1). This can be achieved by an ordinary gauge transformation which takes the momentum into the new operator $p_\phi = (1/i)(d/d\phi) - \theta/2\pi$. The Hamiltonian can now be written as the differential operator

$$H_\theta = -\frac{1}{2}(d/d\phi - i\theta/2\pi)^2 \tag{2.2}$$

with the periodic eigenfunctions $\psi_n(\phi) = (1/2\pi)^{1/2} \exp(in\phi)$. Alternatively, we could have started with the Lagrangian $L_\theta = \frac{1}{2}\dot{\phi}^2 + (\theta/2\pi)\dot{\phi}$ with the canonical momentum $p_\phi = \dot{\phi} + \theta/2\pi$. From $H_\theta = \dot{\phi}p_\phi - L_\theta$ then follows the Hamiltonian (2.2) since now $p_\phi = (1/i)(d/d\phi)$.

We will now investigate the motion of the quantum particle. It is most conveniently done using the path integral formalism for imaginary time $\tau = it$. In particular, we will consider the propagation of the particle from the state $|\phi_0\rangle$ at time $\tau = 0$ to a state $|\phi_T\rangle$ at time $\tau = T$. Dividing the time lapse T into N equal intervals of length $a \rightarrow 0$ such that $Na = T$, one can write the transition amplitude

$$Z_\theta(T) = \langle \phi_T | \exp(-TH_\theta) | \phi_0 \rangle \tag{2.3}$$

as a finite product of infinitesimal amplitudes. They are all of the same form and will be

$$\langle \phi_2 | \exp(-aH_\theta) | \phi_1 \rangle = \frac{1}{2\pi} \sum_{n=-\infty}^{\infty} \exp[i n(\phi_2 - \phi_1) - \frac{1}{2} a(n - \theta/2\pi)^2]$$

when inserting a complete set of energy eigenstates. Now using the Poisson summation formula

$$\sum_{n=-\infty}^{\infty} f(n) = \sum_{q=-\infty}^{\infty} \int_{-\infty}^{\infty} dx f(x) \exp(2\pi i q x) \tag{2.4}$$

and performing the resulting Gaussian integral one finds [6]

$$\begin{aligned} &\langle \phi_2 | \exp(-aH_\theta) | \phi_1 \rangle \\ &= \frac{1}{(2\pi a)^{1/2}} \sum_{q=-\infty}^{\infty} \exp\left(-\frac{1}{2a}(\phi_2 - \phi_1 + 2\pi q)^2 + i(\phi_2 - \phi_1 + 2\pi q)\frac{\theta}{2\pi}\right). \end{aligned} \tag{2.5}$$

Each term in this infinite sum is the exponential of the discretised Lagrangian L_θ corresponding to the particle winding q times around the circle when going from ϕ_1 to ϕ_2 . These angles are compact variables, i.e. defined modulo 2π .

The full transition amplitude can now be written as

$$Z_\theta = \sum_{Q=-\infty}^{\infty} Z_Q \exp(iQ\theta) \tag{2.6}$$

when we drop an irrelevant phase factor $\exp[i(\theta/2\pi)(\phi_N - \phi_0)]$. Here

$$Z_Q = \sum_{\{q_i\}} \int_0^{2\pi} D\phi \exp\left(-\frac{1}{2a} \sum_{i=1}^N (\phi_i - \phi_{i-1} + 2\pi q_i)^2\right) \tag{2.7}$$

is the amplitude for the particle to move from ϕ_0 to ϕ_N with winding number $Q = \sum_{i=1}^N q_i$. The integration measure is $D\phi = (2\pi a)^{-N/2} \prod_{i=1}^{N-1} d\phi_i$.

We can combine the integration over the compact angle ϕ_i with the corresponding local winding number q_i to form a non-compact variable

$$\tilde{\phi}_i = \phi_i + 2\pi \sum_{j=1}^i q_j.$$

The amplitude (2.7) now simplifies to

$$Z_Q = \int_{-\infty}^{\infty} D\tilde{\phi} \exp\left(-\frac{1}{2a} \sum_{i=1}^N (\tilde{\phi}_i - \tilde{\phi}_{i-1})^2\right) \tag{2.8}$$

with $\tilde{\phi}_0 \equiv \phi_0$. It is the amplitude for a free particle to move from ϕ_0 to $\tilde{\phi}_N = \phi_0 + 2\pi Q$ in imaginary time $T = Na$. Integrating, one finds the well known result

$$Z_Q = \frac{1}{(2\pi T)^{1/2}} \exp[-(1/2T)(\phi_N + 2\pi Q - \phi_0)^2] \tag{2.9}$$

which would also have followed more directly from integration of the Schrödinger equation.

We will only need to consider the special case $\phi_N = \phi_0$ where the particle moves a whole number of periods. From (2.6) and (2.9) we then get

$$\begin{aligned} Z_\theta &= \frac{1}{(2\pi T)^{1/2}} \sum_{Q=-\infty}^{\infty} \exp(-2\pi^2 Q^2/T + iQ\theta) \\ &= \frac{1}{(2\pi T)^{1/2}} \Theta_3\left(\frac{\theta}{2\pi}, \frac{2\pi i}{T}\right) \end{aligned} \tag{2.10}$$

as found by Schulman [7]. Here Θ_3 is the Jacobi theta function

$$\Theta_3(z, t) = \sum_{n=-\infty}^{\infty} \exp(i\pi t n^2 + 2\pi i n z). \tag{2.11}$$

Now using the symmetry formula [8]

$$\Theta_3(z, t) = (-it)^{-1/2} \exp(-i\pi z^2/t) \Theta_3\left(\frac{z}{t}, \frac{-1}{t}\right) \tag{2.12}$$

the transition amplitude (2.10) simplifies to

$$Z_\theta = \frac{1}{2\pi} \sum_{n=-\infty}^{\infty} \exp(-E_n(\theta)T) \tag{2.13}$$

with $E_n(\theta) = \frac{1}{2}(n - \theta/2\pi)^2$ being the energy levels of the planar rotor. In this form we recognise this amplitude as the ground-state to ground-state transition amplitude $Z_\theta = \langle \theta(T) | \theta(0) \rangle$ as also follows directly from (2.3) when $\phi_N = \phi_0$.

The two-point correlation function $C_\theta(\tau) = \langle \theta | \phi(\tau) \phi(0) | \theta \rangle$ can easily be calculated. Using $\phi(\tau) = \exp(H_\theta \tau) \phi(0) \exp(-H_\theta \tau)$ and inserting a complete set of energy eigenstates, one has

$$C_\theta(\tau) = \sum_{n=-\infty}^{\infty} |\langle \theta | \phi | n \rangle|^2 \exp[-(E_n - E_\theta)\tau].$$

When $0 \leq \theta < \pi$ the ground state $|\theta\rangle = |0\rangle$. Then $\langle n | \phi | \theta \rangle = i/n$ for $n \neq 0$, $\langle 0 | \phi | \theta \rangle = \pi$ and we find

$$C_\theta(\tau) = \pi^2 + \sum_{n \neq 0} \frac{1}{n^2} \exp[-\frac{1}{2}n(n - \theta/\pi)\tau]. \tag{2.14}$$

A similar expression is obtained when $\pi \leq \theta < 2\pi$. If we choose to parametrise the circle with $\phi \in [-\pi, \pi)$ instead of $\phi \in [0, 2\pi)$ as here, one will find the disconnected piece $|\langle 0 | \phi | \theta \rangle|^2$ to give zero.

In the functional formulation of this problem the correlation function is

$$C_\theta(\tau) = \frac{1}{Z_\theta} \int D\phi \phi(\tau) \phi(0) \exp(-S_\theta[\phi]) \tag{2.15}$$

with the action

$$S_\theta[\phi] = \int_0^T d\tau [\frac{1}{2}\dot{\phi}^2 + (i\theta/2\pi)\dot{\phi}] \tag{2.16}$$

as used previously. Going through the same steps as before we now find that we can write

$$C_\theta(\tau) = \frac{1}{Z_\theta} \sum_{Q=-\infty}^{\infty} C_Q(\tau) Z_Q \exp(iQ\theta) \tag{2.17}$$

where the correlation function $C_Q(\tau) = \langle \phi(\tau)\phi(0) \rangle_Q$ can be expressed as a functionally integrated average over the paths with total winding number Q in analogy with the result in (2.6). The amplitude Z_Q can therefore be interpreted as the probability to find a path with winding number Q in this functional approach.

All quantum mechanical averages can be written as in (2.17). In particular, the expectation value of the kinetic energy $E = -\frac{1}{2}\dot{\phi}^2$ will be the ground-state energy

$$E_\theta = \frac{1}{Z_\theta} \sum_{Q=-\infty}^{\infty} E_Q Z_Q \exp(iQ\theta) \tag{2.18}$$

when the averages are taken over paths with $T \rightarrow \infty$. In order to get a finite result in the limit $a \rightarrow 0$, one must regularise this result, since the velocity $\dot{\phi}$ is not finite. This can be done as explained by Feynman and Hibbs [9] by taking the product $\dot{\phi}^2$ at two different times separated by a distance a which is then taken to zero:

$$E_Q = -\frac{1}{2a^2} \langle (\phi_{i+1} - \phi_i)(\phi_i - \phi_{i-1}) \rangle_Q. \tag{2.19}$$

We will explicitly make use of this formula in § 4 where the quantum problem is investigated in a Monte Carlo simulation.

It is possible to calculate E_Q directly. Inverting (2.18) one can write it as a Fourier transform of $E_\theta Z_\theta$. In the limit $T \rightarrow \infty$ one finds from the partition function (2.13) that

$$E_\theta = -\frac{d}{dT} \ln Z_\theta. \tag{2.20}$$

With this in the Fourier integral one obtains

$$E_Q = -\frac{d}{dT} \ln Z_Q \tag{2.21}$$

in the same limit. With Z_Q from (2.9) where now $\phi_0 = \phi_N$ we get immediately

$$E_Q = \frac{1}{2T} - \frac{2\pi^2 Q^2}{T^2}. \tag{2.22}$$

The dependence on the winding number for large times T is very slow since Q appears only in the term of order $1/T^2$. Except for a difference in sign, the functional form of E_Q is quite similar to what Bhanot *et al* [2] found in a Monte Carlo simulation of four-dimensional SU(2) lattice gauge theory.

3. Quantum paths as random walks

A method to compute Z_θ numerically presents itself through (2.9), where the amplitude Z_Q can be interpreted as the probability for a Brownian particle with diffusion constant $D = \frac{1}{2}$ to move from ϕ_0 to ϕ_N in time T . Again we choose $\phi_N = \phi_0$. This Brownian motion can be approximated by a symmetric random walk with the same probability

$\frac{1}{2}$ to jump a distance $\Delta = \sqrt{a}$ to the left or to the right. Obviously, this analogy should be expected since with imaginary time the Schrödinger equation for zero potential is just the diffusion equation. The velocity at each step from the point ϕ_i to ϕ_{i+1} will simply be the angular difference Δ divided by the lattice constant a . This approximation leaves the action constant equal to $S = \frac{1}{2}N$ and all paths have the same weight.

One can easily extend this correspondence between quantum motion and random walks to also include non-zero potentials [10]. In fact, it forms the basis of the so-called random walk Monte Carlo algorithm which can be used to obtain non-perturbative numerical results for much more complex quantum systems like liquid helium [11] and lattice gauge theories [12]. A quantum particle on a circle is probably the simplest non-trivial example where the essence of this powerful method can be most easily demonstrated.

We can now actually calculate the ground-state energy of the quantum particle moving on a finite lattice of length $T = Na$ in the imaginary time direction. At every step in this direction the particle will move with equal probability a step $\Delta = \sqrt{a}$ to the right or to the left on the circle which is partitioned into M intervals such that $M\Delta = 2\pi$. Of all the 2^N random walks of N steps there are

$$P_m^N = \binom{N}{\frac{1}{2}(N-m)} \tag{3.1}$$

with a net displacement $m\Delta$ along the circle. These particular walks will, in analogy with (2.19), have an average energy

$$E_m = -\frac{1}{2a^2} \langle (\phi_{i+1} - \phi_i)(\phi_i - \phi_{i-1}) \rangle_m \tag{3.2}$$

but now with $|\phi_i - \phi_{i-1}| = \Delta$. Looking at the $N - 1$ interior sites of the time lattice, we see that at B sites there is a change of direction in the random walk, i.e. a break. At the remaining $S = N - 1 - B$ sites it continues in the same direction. We can then simplify (3.2) to

$$E_m = -\frac{\Delta^2}{2a^2(N-1)} [N - 1 - 2\langle B \rangle_m]. \tag{3.3}$$

In order to calculate the average $\langle B \rangle_m$ we need an expression for the number of paths with a definite number of breaks, ending a distance $m\Delta$ from the starting point. Thus we will be able to give each term contributing to E_m the appropriate weight.

In order to find this combinatorial factor we will follow Jacobson and Schulman [13] in their investigation of the one-dimensional Dirac equation, referring to the path drawn in figure 2. Here $R = \frac{1}{2}(N + m)$ is the total number of steps to the right, and $L = \frac{1}{2}(N - m)$ is the corresponding number of steps to the left. On the tilted frame encompassing the path in the figure we project on the lower right side the sections of the path having steps only to the right. The steps to the left are projected on the lower left side. We see that for paths starting with a right step and ending with a left step, the number B of breaks will be odd. There will be a total number of $\frac{1}{2}(B - 1) + 1$ left breaks and $\frac{1}{2}(B - 1)$ right breaks. The number of paths satisfying this requirement is obtained by distributing the left breaks minus the compulsory last one among the steps to the right minus the first compulsory one, i.e. we distribute $\frac{1}{2}(B - 1)$ left breaks among $R - 1$ right steps. Independently, we distribute the right breaks among the left steps,

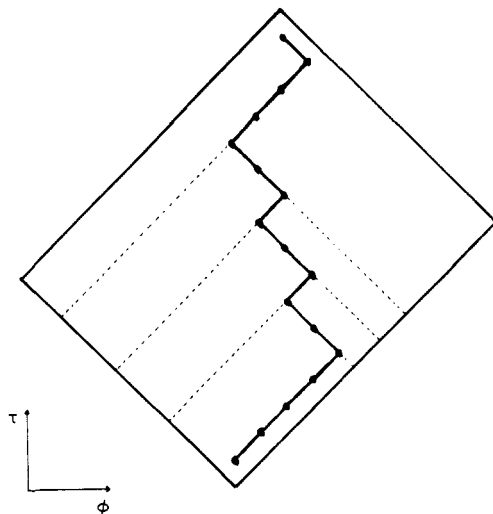


Figure 2. Paths generated by a random walk with $N = 16$ steps, $B = 7$ breaks and $R = 9$ right steps which is a contribution to P_{RL} in the text.

omitting the last compulsory step. Thus the number of paths of this kind will be

$$P_{RL} = \binom{R-1}{\frac{1}{2}(B-1)} \binom{L-1}{\frac{1}{2}(B-1)}.$$

Following this reasoning we find the same number of paths with compulsory first left and last right steps, i.e. $P_{LR} = P_{RL}$.

Next we look at paths starting out and coming in with right steps. The total number of breaks will now be even, with $\frac{1}{2}B$ breaks both to the left and to the right. Due to the compulsory first and last steps we find the total numbers of such paths to be

$$P_{RR} = \binom{R-1}{\frac{1}{2}B} \binom{L-1}{\frac{1}{2}B-1}.$$

Similarly we have for paths starting and coming in with left steps

$$P_{LL} = \binom{R-1}{\frac{1}{2}B-1} \binom{L-1}{\frac{1}{2}B}.$$

These expressions yield the total number of paths $P_{m,B}^N$ with N steps in the time direction, a net displacement of m spatial steps and with B breaks. When B is odd, it will be $P_{m,B}^N = 2P_{RL}$, and for B even $P_{m,B}^N = P_{RR} + P_{LL}$. These results can now be combined into

$$P_{m,B}^N = \binom{R-1}{[\frac{1}{2}B]} \binom{L-1}{[\frac{1}{2}(B-1)]} + \binom{R-1}{[\frac{1}{2}(B-1)]} \binom{L-1}{[\frac{1}{2}B]} \tag{3.4}$$

where $[k]$ denotes the greatest integer less than or equal to k . Summing over all breaks B we must have for consistency that

$$\sum_{B=0}^{N-1} P_{m,B}^N = P_m^N \tag{3.5}$$

as is verified in the appendix.

The expectation value

$$\langle B \rangle_m = \frac{1}{P_m^N} \sum_{B=0}^{N-1} B P_{m,B}^N \tag{3.6}$$

which is needed in (3.3) can now be calculated. After some further manipulations of the binomial coefficients which are found in the appendix we find

$$\langle B \rangle_m = \frac{1}{2}(N - m^2/N). \tag{3.7}$$

Inserting this result into (3.3) the average energy is found to be

$$E_m = \frac{\Delta^2}{2a^2(N-1)} \left(1 - \frac{m^2}{N} \right) \tag{3.8}$$

for those paths with a net displacement of $m\Delta$.

In the special case with closed trajectories the displacement is given by the winding number Q as $m\Delta = 2\pi Q$. We can now take the continuum limit $a \rightarrow 0$, $N \rightarrow \infty$ for finite $T = Na$. From (3.1) we can then easily find the probability to have a closed trajectory with winding number Q . It is $2^{-N} P_m^N \rightarrow (2/\pi N)^{1/2} \exp[-(2\pi Q)^2/2N\Delta^2]$ which is essentially Z_Q given in (2.9) as expected. Similarly, in the same limit, the energy (3.8) is just the continuum result (2.22) as is easily seen using $\Delta^2 = a$.

We can now find the θ -dependent ground-state energy of the discretised problem by inserting (3.8) and (3.1) into (2.18) with $m = MQ$. A typical result is shown in figure 3 when the circle is divided into $M = 14$ segments, and with walks of $N = 100$ steps in the time direction. For comparison we have also shown the exact result in the continuum limit $a \rightarrow 0$. When θ is close to 0 or 2π the different sums converge fast and we find energies close to the exact continuum results. For this choice of parameters we get $E_{\theta=0} \approx 10^{-4}$ as compared to the exact result, which is zero. On the other hand, when θ is close to π the results are not so accurate. Then all the oscillatory terms in Z_θ are found to add up to a small quantity. This behaviour can be understood since the system experiences level crossing at $\theta = \pi$. Hence the ground state is more difficult to isolate in this region. Similarly the numerator in (2.18) also becomes small for the

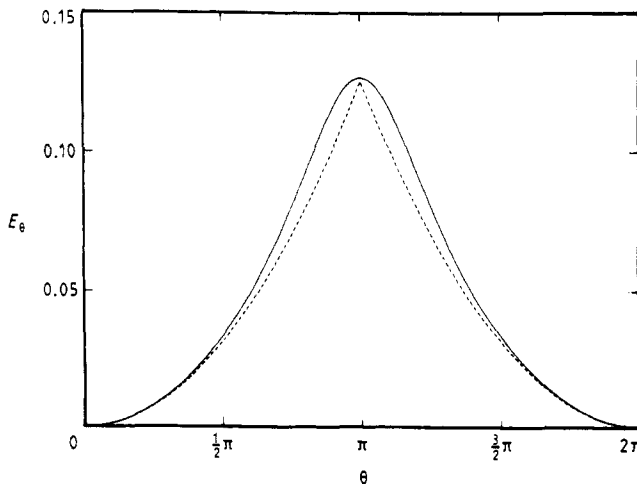


Figure 3. Ground-state energy of the discretised planar rotor. The broken curve gives the continuum result.

same reason. The ground-state energy being the ratio of these two functions therefore requires higher accuracy in this region.

This solution for a finite lattice approaches the continuum limit more closely as M decreases. However, then the cancellation mentioned above becomes more severe, until for $M = 2$ the energy E_θ becomes indefinite at $\theta = \pi$. Then both numerator and denominator become exactly zero as shown in the appendix. Expanding the numerator and denominator around $\theta = \pi$ one can isolate the leading term $(4/a)(\theta - \pi)^{-2}$ in the ratio showing that $E_{\theta=\pi}$ is in fact infinite in this special case.

4. Random walk Monte Carlo simulations

In lattice versions of non-Abelian gauge theories one cannot calculate the θ -dependent vacuum energies as we have for the planar rotor. The only way to find this non-perturbative dependence seems to be by Monte Carlo simulations. This has been done by Bhanot *et al* [2] using the Metropolis algorithm to investigate four-dimensional SU(2) gauge theories. One is then faced with an additional problem of how to relate this θ dependence on a finite lattice to what we would have in the continuum version of the theory. It is therefore of interest to see how our results for the planar rotor on a lattice can be obtained from Monte Carlo simulations and how well these results compare with the exact results in the continuum limit.

The action (2.16) has an imaginary term and thus cannot be used right away in a Monte Carlo simulation based on the Metropolis or heat bath algorithms. This problem can easily be avoided by first calculating expectation values $\langle A(\phi) \rangle_Q$ from configurations of the planar rotor corresponding to definite topological charge or winding number Q and then summing all these contributions with a complex weight $Z_Q \exp(iQ\theta)$ as in (2.17). The amplitude Z_Q is proportional to the probability of finding a configuration in imaginary time. Both Z_Q and $\langle A(\phi) \rangle_Q$ are straightforward to find from such simulations.

For this problem a faster and more natural algorithm follows from the random walk approximation to the quantum motion of the particle as discussed in the previous section. Since the action is the same for all such walks with the same number of steps in the time direction, an average of a quantity $A(\phi)$ over walks with winding number Q will then simply be

$$\langle A(\phi) \rangle_Q = \frac{1}{Z_Q} \sum_{r \in Q} A(\phi_r) \tag{4.1}$$

where the index r denotes different walks in this topological class. The quantum amplitude Z_Q is then proportional to the number of walks in the class, i.e.

$$Z_Q = \sum_{r \in Q} 1. \tag{4.2}$$

From here follows Z_θ directly from (2.6). The physical expectation value $\langle A(\phi) \rangle_\theta$ is now obtained from

$$\langle A(\phi) \rangle_\theta = \frac{1}{Z_\theta} \sum_Q \langle A(\phi) \rangle_Q Z_Q \exp(iQ\theta) \tag{4.3}$$

in analogy with (2.17) for the correlation function.

The energy of the ground state is found from this Monte Carlo simulation using (2.19) for the kinetic energy. In figure 4 we show the result based on 100 000 random

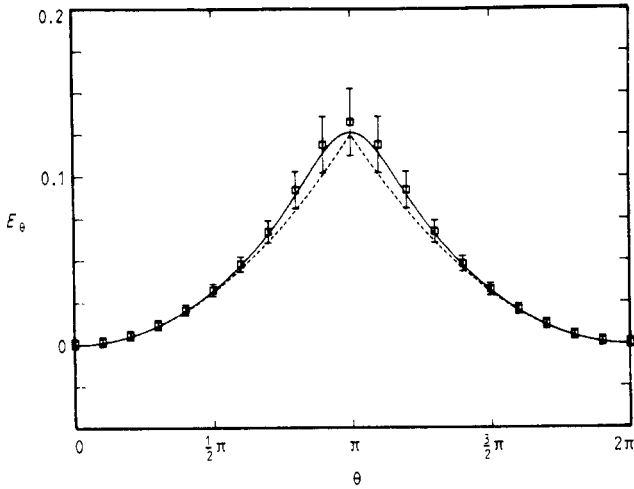


Figure 4. Results for the ground-state energy for the discretised planar rotor obtained from a simulation based on 100 000 random walks, each with $N = 100$ steps and $M = 14$ intervals on the circle. CPU time is 2 min on a ND-570 minicomputer.

walks generated on a lattice with $N = 100$ points and with the circle divided into $M = 14$ segments. Here we have given error bars based on the variations in the measurements grouped into ten runs each with 10 000 random walks. The calculated points and corresponding error bars are seen to fall rather smoothly along the theoretical curve. This is to be expected since they are all obtained from the same set of generated random walks. The small discrepancy between these simulated values and the exact result calculated in the previous section is due to fluctuations. It decreases when the generated number of random walks is made larger, and is zero when this number becomes infinite.

When larger values of M are used for the same lattice size N , the maximal attainable value for the winding number Q becomes smaller. This results in good statistics for the measured observables and good determination of Z_Q . Even for θ near π the simulation converges quickly. The calculation in § 3 shows however that the limit of convergence is relatively far from the continuum result, i.e. the finite-size effect is more pronounced. On the other hand, if M is taken to be smaller, the approach to the continuum limit is faster since the lattice spacing a and thereby the time T grows. This serves to isolate the continuum ground state better. But the uncertainties in the measurements are larger, especially for higher values of Q . For θ in the region close to π the different sums over Q exhibit large cancellations as discussed in the previous section. Thus the error accumulates, producing larger fluctuations in this region of θ .

In principle it is possible to obtain higher energy levels from this simulation by calculating accurately higher correlation functions. The first excited state can be isolated in the two-point correlation function (2.14) in the limit where the point separation $\tau \rightarrow \infty$. It is here convenient to parametrise the circle by $\phi \in [-\pi, \pi)$ so that the disconnected piece is zero. Then the energy difference $\Delta E_\theta = E_1(\theta) - E_0(\theta)$ is given by

$$\Delta E_\theta = -\frac{d}{d\tau} \ln C_\theta(\tau)|_{\tau \rightarrow \infty} \quad (4.4)$$

and seen to equal $\Delta E_\theta = \frac{1}{2}(1 - \theta/\pi)$ in the interval $0 \leq \theta < \pi$.

We show in figure 5 results for the correlation function for three values of θ obtained from simulations on the same lattice. One notices that these points for large values of the argument τ fall approximately on straight lines as they should. In addition they should also meet at $\tau = 0$ at the point $C_\theta(\tau = 0) = \frac{1}{3}\pi^2$. The reason why they fail to do so is due to the finite size of the lattice; they will approach this continuum value when $a \rightarrow 0$.

The energy difference ΔE_θ can now be found from (4.4), and the results are shown in figure 6. The points should fall on the straight line $\Delta E_\theta = \frac{1}{2}(1 - \theta/\pi)$ as they are roughly seen to do when $0 \leq \theta < \pi$. One can easily make the agreement with the

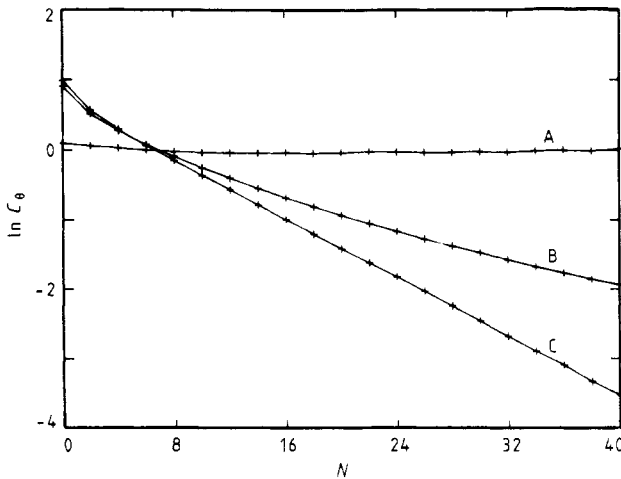


Figure 5. Logarithm of the two-point correlation function for three values of θ where the point separation is given by the number N of lattice units ($\theta = \pi$ (A), $\pi/2$ (B), 0 (C)). The measured values are based on a simulation with 100 000 random walks on the same lattice as in figure 4, now requiring a CPU time of approximately 9 min.

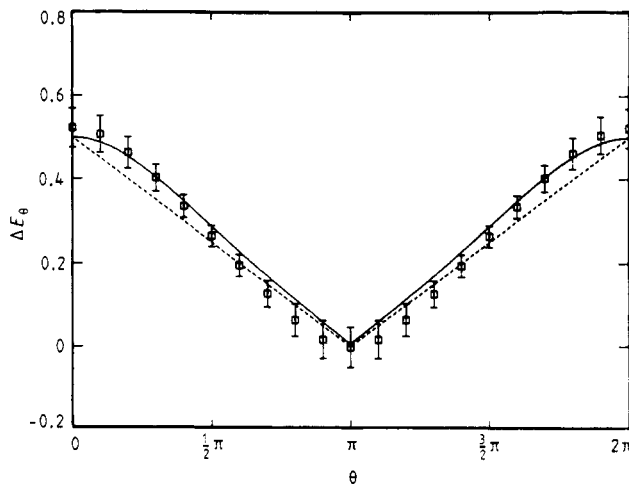


Figure 6. Energy gap obtained from the correlation function in figure 5. The full curve is the expected result for finite time separation, while the broken line is the exact result in the continuum limit.

continuum results better by using a larger lattice which allows for larger separation τ . As long as τ is finite, there will also be contributions to the correlation function $C_\theta(\tau)$ from higher states as seen from (2.14). Taking into account the next higher state with quantum number $n = -1$ one finds

$$C_\theta(\tau) = 2 \exp(-\frac{1}{2}\tau) \cosh(\theta\tau/2\pi). \tag{4.5}$$

Obtaining the energy difference from the slope formula (4.4) one finds

$$\Delta E_\theta = \frac{1}{2}[1 - (\theta/\pi) \tanh(\theta\tau/2\pi)] \tag{4.6}$$

with θ in the same interval as before. This corrected energy difference is seen to approach the exact result in the limit $\tau \rightarrow \infty$. It is also shown in figure 6 and is seen to agree with the simulated points.

The difficulties in isolating the energy gap are more pronounced for small values of θ . On the other hand, when θ approaches π we get larger fluctuations due to uncertainties in Z_Q and poor statistics in C_Q for large Q values. Both of these difficulties can be eliminated by adding a periodic potential $V(\phi)$ to the problem, lifting the degeneracies. Expectation values $\langle A(\phi) \rangle_\theta^V$ are then again related to $\langle A(\phi) \rangle_Q^V$ exactly as for zero potential [6]. Choosing a potential $V(\phi) = \lambda(1 - \cos \phi)$ with λ small we can then use the same Monte Carlo algorithm based on random walks. The only difference will be that now the walker feels the potential which must be included in the averages. Adding the potential to the action (2.16) we see that it will give the modified expectation value

$$\langle A(\phi) \rangle_Q^V = \left\langle A(\phi) \exp\left(-\int_0^T d\tau V[\phi(\tau)]\right) \right\rangle_Q \tag{4.7}$$

where the right-hand side is the average taken over free random walks [10]. It can again be obtained from simulations using (4.1).

The simulated results for the ground-state energy E_θ and the energy gap ΔE_θ for $\lambda = 0.4$ are shown in figures 7 and 8. For the same number of random walks generated

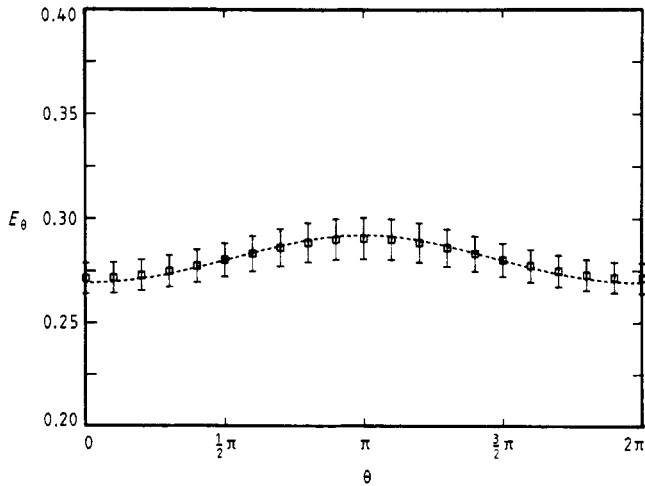


Figure 7. Ground-state energy of the discretised planar rotor in a non-zero potential with $\lambda = 0.4$. These results are based on the same lattice and from the same number of random walks as before.

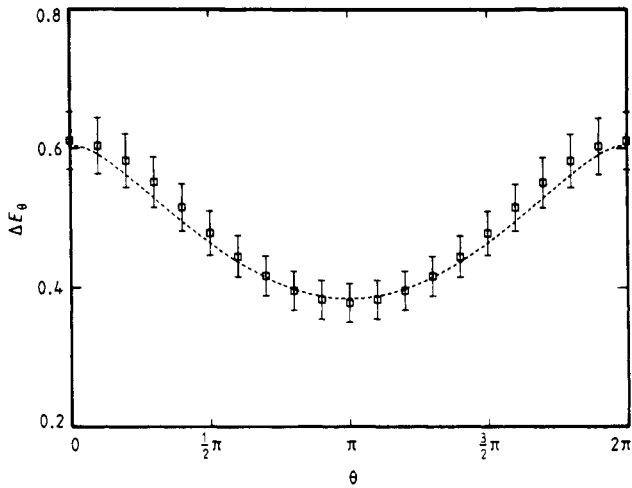


Figure 8. Energy gap for a planar rotor in a non-zero potential with $\lambda = 0.4$ on the same lattice and from the same number of random walks as previously.

previously and the same lattice we find better agreement with the continuum results, which are also shown in the figures. These are obtained from directly diagonalising the Hamiltonian in a finite basis of plane waves $\exp(in\phi)$. For $\theta = 0$ the energy levels are directly given by the eigenvalues of the Mathieu equation.

When the coupling constant λ becomes large it is obvious that most of the generated random walks will give small or negligible contributions to the averages (4.7) because of the exponential of the potential. This particular Monte Carlo algorithm is then no longer very efficient but can easily be improved by generating so-called guided random walks [10, 12] which try to keep the particle away from the classically inaccessible regions. One can use this modified algorithm to investigate the instantons which appear in this model when the coupling constant λ becomes sufficiently large [14].

5. Conclusion

The planar rotor is the simplest quantum model which is topologically non-trivial and which exhibits a θ dependence of the same kind as is expected in non-Abelian gauge theories like QCD. In the lattice version of this simple system, the topological charge is given directly by the winding number of the particle on the discretised circle. On the other hand, for a gauge theory on a lattice it is not so obvious how to define a topological charge which also can be taken consistently into the continuum limit.

It would be of interest to find out if the concept of paths in the topologically non-trivial configuration spaces of gauge theories could be used to get a better understanding of the appearance of topological quantum numbers in some of these theories. If that were the case, then it would be very natural to try to extract this information and thereby also the θ dependence of physical quantities from Monte Carlo simulations based on the random walk algorithm. For the planar rotor we have found it to be pretty near ideal.

Appendix

The average $\langle B \rangle_m$ in (3.6) can be obtained from the addition theorem of binomial coefficients [15]. It can be derived from the identity

$$(a + b)^n(c + d)^m = \sum_{r=0}^n \sum_{s=0}^m \binom{n}{r} \binom{m}{s} a^r b^{n-r} c^s d^{m-s} \tag{A1}$$

when setting $a = c$ and $b = d$ on both sides and identifying products of powers $a^p b^q$. One finds

$$\sum_{p=0}^k \binom{n}{p} \binom{m}{k-p} = \binom{n+m}{k}. \tag{A2}$$

In addition we will need sums which can be obtained from taking the derivative with respect to a on both sides of (A1). Again setting $a = c$ and $b = d$ we then get

$$\sum_{p=1}^k p \binom{n}{p} \binom{m}{k-p} = n \binom{n+m-1}{k-1} \tag{A3}$$

when using (A2). More complicated sums can be obtained by taking higher derivatives. Changing variables in the summation formula (A2) it can be shown to give

$$\sum_{p=0}^n \binom{n-\frac{1}{2}m}{p} \binom{n+\frac{1}{2}m}{p} = \binom{2n}{n-\frac{1}{2}m} \tag{A4}$$

$$\sum_{p=1}^n \binom{n-\frac{1}{2}m}{p} \binom{n+\frac{1}{2}m}{p-1} = \binom{2n}{n-\frac{1}{2}m-1}. \tag{A5}$$

Using these two sums it is straightforward to verify the normalisation (3.5).

The expectation value (3.6) follows from (A3) after changing variables. One can then derive that

$$\sum_{p=1}^n p \binom{n-\frac{1}{2}m}{p} \binom{n+\frac{1}{2}m}{p} = (n-\frac{1}{2}m) \binom{2n-1}{n-\frac{1}{2}m} \tag{A6}$$

$$\sum_{p=1}^n p \binom{n-\frac{1}{2}m}{p} \binom{n+\frac{1}{2}m}{p-1} = (n-\frac{1}{2}m) \binom{2n-1}{n+\frac{1}{2}m}. \tag{A7}$$

In actual calculations $n = \frac{1}{2}N - 1$. We have here assumed N even. Putting all this together we can finally write down the desired result (3.8).

When $M = 2$ we have $m = 2Q$ and the energy becomes

$$E_Q = \frac{\Delta^2}{2a^2(N-1)} \left(1 - \frac{4Q^2}{N} \right). \tag{A8}$$

When this expression is used in (2.18) at the special value $\theta = \pi$ the denominator will be the partition function

$$Z_\theta = 2 \sum_{Q=1}^{N/2} (-1)^Q \binom{N}{\frac{1}{2}N - Q} + \binom{N}{\frac{1}{2}N}. \tag{A9}$$

The numerator will take the similar form

$$\frac{\Delta^2}{2a^2(N-1)} \left[2 \sum_{Q=1}^{N/2} \left(1 - \frac{4Q^2}{N} \right) \binom{N}{\frac{1}{2}N - Q} (-1)^Q + \binom{N}{\frac{1}{2}N} \right]. \tag{A10}$$

We can now show that both of these expressions equal zero. Actually we have that

$$2 \sum_{Q=1}^{N/2} (-1)^Q Q^k \binom{N}{\frac{1}{2}N - Q} = 0 \tag{A11}$$

for $k = 2, 4, \dots, N - 2$. This can be shown from the identity

$$x^{-n}(1-x)^{2n} = \sum_{q=0}^{2n} (-1)^q \binom{2n}{q} x^{q-n} \tag{A12}$$

and operating on both sides p times with $D \equiv x d/dx$. After some rearrangements one can compare terms on both sides and find

$$2 \sum_{q=1}^n (-1)^q \binom{2n}{n-q} q^p + \binom{2n}{n} \delta_{p,0} = 0 \tag{A13}$$

for $p = 0, 2, \dots, 2n - 2$. With $n = \frac{1}{2}N$, $q = Q$ and $p = 0$ this just gives $Z_\theta = 0$, as can be seen from (A9). When $p = 2$ we now see that the expression in (A10) also is zero.

For all partitions $M > 2$ of the circle there is no such singularity for $\theta = \pi$ on the finite lattice. The divergence of $E_{\theta=\pi}$ can be isolated by a Taylor expansion. One will then also need (A13) for the higher powers of p .

References

- [1] Coleman S 1977 *The Whys of Subnuclear Physics* ed A Zichichi (New York: Plenum)
- [2] Bhanot G, Rabinovici E, Seiberg N and Woit P 1984 *Nucl. Phys. B* **230** 291
- [3] Asorey M, Esteve J G and Pacheco A F 1983 *Phys. Rev. D* **27** 1852
- [4] Lin C C and Swalen J D 1959 *Rev. Mod. Phys.* **31** 841
- [5] Peshkin M 1981 *Phys. Rev. A* **23** 360
- [6] Bunk B and Wolff U 1983 *Nucl. Phys. B* **215** 495
- [7] Schulman L S 1981 *Techniques and Application of Path Integration* (New York: Wiley)
- [8] Courant R and Hilbert D 1953 *Methods of Mathematical Physics* vol I (New York: Interscience)
- [9] Feynman R P and Hibbs A R 1965 *Quantum Mechanics and Path Integrals* (New York: McGraw-Hill)
- [10] Barnes T and Daniell G J 1985 *Nucl. Phys. B* **257** 173
- [11] Kalos M H, Lee M A, Whitlock P A and Chester G V 1981 *Phys. Rev. B* **24** 115
- [12] Chin S A, Negele J W and Koonin S E 1984 *Ann. Phys., NY* **157** 140
- [13] Jacobson T and Schulman L S 1984 *J. Phys. A: Math. Gen.* **17** 375
- [14] Fjeldsø N and Ravndal F 1988 in preparation
- [15] Margenau H and Murphy G M 1959 *The Mathematics of Physics and Chemistry* (New York: Van Nostrand)